

Interactive
comment

Interactive comment on “A relation between the locations of the polar boundary of outer electron radiation belt and the equatorial boundary of the auroral oval” by Maria O. Riazantseva et al.

Maria O. Riazantseva et al.

orearm@gmail.com

Received and published: 11 April 2018

This paper presents potentially interesting results and interpretations. With a little more detail within the manuscript, and slightly more interaction between the introduction and the conclusions sections it will provide a useful scientific step forward. Some comments regarding the text and figures are presented below:

We are grateful for your careful reading of our paper! We try to improve the paper taking into account all your comments.

1) In the paragraph starting page 2, Line 19 two mechanisms are put forward for the

[Printer-friendly version](#)

[Discussion paper](#)



relative locations of the equatorial boundary of the auroral oval and the outer radiation belt trapping boundary. The rest of the paper is about determining which mechanism is supported by the analysis of satellite data as presented. However, the opening sentence of page 8, line 18 indicates that the results agree with Anotonova et al. 2017. This work was not mentioned in the Introduction section and therefore is not expected. The new work should be discussed in section 1 to give the reader the background to the research mentioned in that paper.

The main idea presented in this study rose once it became clear that the main part of the auroral oval is not mapped onto the plasma sheet, as it used to be widely accepted. According to our previous studies, the oval is mapped onto the surrounding-the-Earth plasma ring. The existence of such ring, which exhibits characteristics similar to the plasma sheet, was known from the first satellite plasma measurements (see, for example, (Frank, 1971, doi:10.1029/JA076i010p02265). Transverse currents in this ring are closed inside the magnetosphere. So we added a discussion of the results by Anotonova et al.(2017) in the Introduction p.2 .l.24-25

2) The first paragraph of section 1 discusses the L-shell variations of the boundaries, particularly the outer radiation belt trapping boundary. Given the use of 100 keV in this study to determine the boundary location rather than 40 keV or 35 keV as previously used, it would be beneficial to the paper if the distributions in L-shell of the boundaries were plotted for the whole dataset - similar to Figures 4 and 5. These new figure(s) would provide clarity for the reader and confirm that the algorithm is producing results that are consistent with the previous work cited in paragraph 12, section 1.

Thank you for your comment! We use the lowest channel of energetic electrons (>100 keV) available on Meteor-M1 satellite to determine the trapping boundary. Below we show plots (figure 2.1) of the probability distributions of finding the obtained boundaries for each L value (where L is McIlwain parameter). For quiet geomagnetic condition the average value of the polar boundary of the ORB $\approx 8 \pm 1$, the average value of the equatorial auroral oval boundary is almost the same $\approx 8 \pm 2$. For perturbed geomagnetic



condition $AE > 150$ nT the average value of the polar boundary of the ORB is also $\approx 8 \pm 1$, whereas the average value of the equatorial auroral oval boundary is much less $\approx 6 \pm 2$. The average position of the polar boundary of the ORB agrees with the position of the trapping boundary published by Vernov et al. (2009). We added figures and comments in section 3 p.9. I.3-9

3) Figures 4 and 5 show the distributions of the boundaries for northern and southern hemispheres. However, no obvious follow-up of this separation is undertaken, and it is unclear why it is done. It is reasonable to use the PCS index for the southern hemisphere analysis, but it is unclear why the data continue to be separated hemispherically after that. Just having one plot for each activity index would clarify the presentation and aid the discussion of the main result, i.e., that there is a latitudinal difference in the distributions for quiet and active conditions.

The maximums of distributions of ΔLat for northern and southern hemispheres (see the figure 2.2 below) are slightly different (in adjacent bins). The combined distribution, for both hemispheres, exhibits a smeared maximum, and the effect is less clear. During the data analysis we found important differences using the AE and the PC indexes. The AE index is produced only due to magnetic measurements in the northern hemisphere. At the same time, the PC index exists separately for northern and southern hemispheres. We obtain slightly different pictures of ΔLat for both hemispheres. We do not know whether this effect is connected to the difference in magnetic field between both hemispheres (IGRF effect) or some kind of seasonal effect (our measurements were made on September 2009 - April 2010). It could be very interesting to clarify this subject in the future. This is why we prefer to publish our figures without averaging both hemispheres.

Some small points:

4) 'to the equator of' should be replaced by 'equatorward of'. 'to the pole of' should be replaced by 'poleward of'.

[Printer-friendly version](#)

[Discussion paper](#)



Thank you! We have corrected the terms everywhere.

5) Page 2, line 4-5. The sentence is unclear. I think it says that the outer radiation belt trapping boundary is clearly identifiable in low orbiting satellite data.

Thank you! We have corrected this sentence. (p. 2 l.2-3.)

6) It would be useful to the reader to state whether the electron detector was measuring spin averaged electrons or was omni-directional etc.

Unfortunately, we have no information on the pitch-angle distribution of both auroral electrons and energetic electrons. METEOR-1 satellites were spin stabilized. The detectors of GGAK-M instrument look within the loss cone and mostly observe precipitating particles. However, because of the large fields of view and particle scattering, some amount of the trapped population is also seen. We used early published information about the isotropy of the observed fluxes of energetic electrons near the ORB from Imhof et al. (1990, 1991, 1992, 1993). Auroral oval was identified by precipitating low energy electrons.

7) Page 4, line 7-8. What energy did you use to calculate the average value and std of the electron fluxes? Same question for the total energy electron flux. If all of the auroral electron energy data in the range from 0.032-16.64 keV was used, how was it combined?

The polar boundary of ORB was determined using the average flux of electrons with energy >100 keV. The equator boundary of the auroral oval was determined using the value of the total energy flux of low energy electrons. Each spectra was approximated in the range 0.032-16.64 keV with an energy step $d\epsilon = 0.01$ keV, and the energy flux was calculated as a numerical integral

$$Flux_\epsilon = 2\pi \int (j(\epsilon) \cdot \epsilon d\epsilon) \quad (1)$$

($j(\epsilon)$ - flux for current value of energy ϵ). We have added the corresponding explanation C4

Interactive comment

[Printer-friendly version](#)

[Discussion paper](#)



tions in the text (p. 4 l.10-13).

8) Figure 1. The caption should describe the lines added to the plot. What does the red vertical dashed line represent. The caption should say - the text doesn't. Why are there two green vertical lines at 14:06 UT. Why is there a red vertical line in Figure 1 and a blue vertical line in Figure 2?

We are sorry. I. The new version contains corrected and improved figures 1-3.

Please also note the supplement to this comment:

<https://www.ann-geophys-discuss.net/angeo-2018-6/angeo-2018-6-AC3-supplement.zip>

Interactive comment on Ann. Geophys. Discuss., <https://doi.org/10.5194/angeo-2018-6>, 2018.

[Printer-friendly version](#)

[Discussion paper](#)



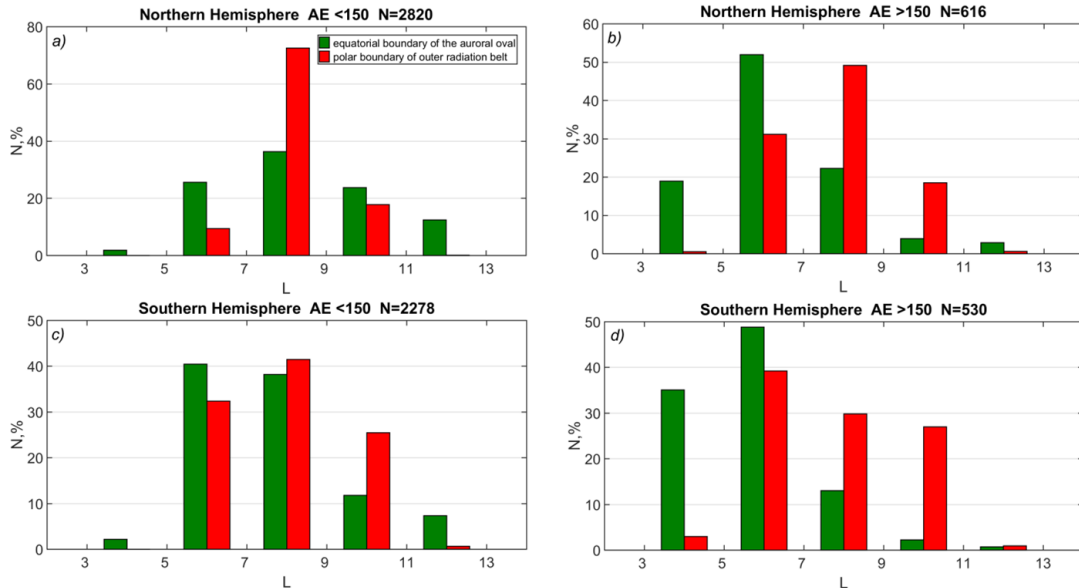


Figure 2.1: The distributions of the position of equatorial boundary of the auroral oval (green bins) and the polar ORB boundary (red bins) from the L (where L is the McIlwain parameter) for northern (a,b) and southern (c,d) hemispheres for AE < 150 nT (a,c) and AE > 150 nT (b,d).

Fig. 1.

[Printer-friendly version](#)

[Discussion paper](#)



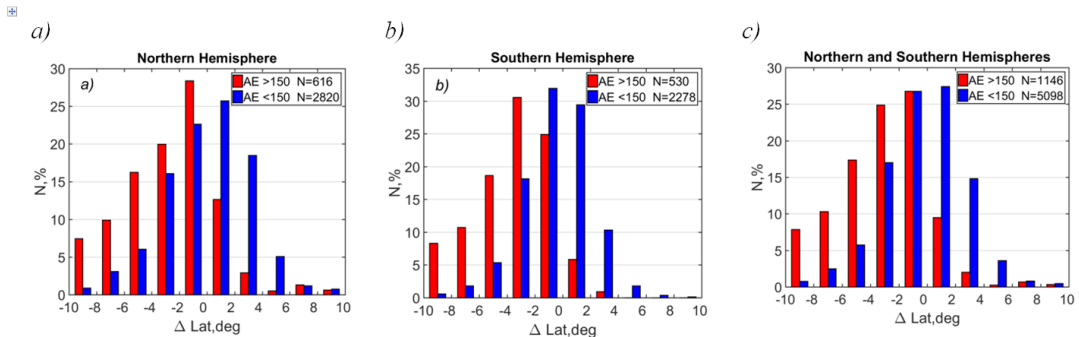


Figure 2.2: The distribution of ΔLat for $\text{AE} > 150 \text{ nT}$ (red bins) and $< 150 \text{ nT}$ (blue bins) for northern (a) and southern (b) and combined northern and southern (c) hemispheres

Fig. 2.

Printer-friendly version

Discussion paper

